Wind and Structures, Vol. 8, No. 5 (2005) 373-388
DOI: http://dx.doi.org/10.12989/was.2005.8.5.373

Aeroelastic forces on yawed circular cylinders: quasi-steady modeling and aerodynamic instability

Luigi Carassale†, Andrea Freda‡ and Giuseppe Piccardo‡†

Dipartimento di Ingegneria Strutturale e Geotecnica, University of Genova, Via Montallegro 1, 16145 Genova, Italy

(Received August 4, 2005, Accepted May 5, 2005)

Abstract. Quasi-steady approaches have been often adopted to model wind forces on moving cylinders in cross-flow and to study instability conditions of rigid cylinders supported by visco-elastic devices. Recently, much attention has been devoted to the experimental study of inclined and/or yawed circular cylinders detecting dynamical phenomena such as galloping-like instability, but, at the present state-of-the-art, no mathematical model is able to recognize or predict satisfactorily this behaviour. The present paper presents a generalization of the quasi-steady approach for the definition of the flow-induced forces on yawed and inclined circular cylinders. The proposed model is able to replicate experimental behaviour and to predict the galloping instability observed during a series of recent wind-tunnel tests.

Keywords: quasi-steady modeling; aerodynamic instability; yawed cylinders; galloping.

1. Introduction

The development of mathematical models for simulating wind loads on moving structures is a fundamental topic in wind engineering. The quasi-steady hypothesis has been often adopted due to its simple derivation and application, mainly for the cases of flow perpendicular to the structural span. A more general approach is desirable since structures (or structural elements) are often in a very generic position with respect to the wind, with both incidence and yaw angles different than zero. Unfortunately, the aerodynamics of yawed cylinders, having strongly three-dimensional characteristics, is much more complicate than the usual case of cross-flow. Matsumoto, *et al.* (1990) studying the wind-rain instability of (yawed) circular cylinders observed the existence of an intense secondary axial flow whose sole presence could give rise to unstable oscillations even without water rivulet. Recently a wide experimental campaign on cable models has been carried out at the National Research Council of Canada (NRC), in collaboration with Rowan Williams Davies and Irwin Inc. (RWDI) and the University of Ottawa (Cheng, *et al.* 2003a, Cheng, *et al.* 2003b, Larose, *et al.* 2003). The aerodynamic behaviour of dry, non-iced, smooth cables against skew wind has been examined by a series of dynamic and static experiments recognizing cases of divergent oscillations for some combinations of cable inclination and yaw angle.

† Assistant Professor, Corresponding Author, E-mail: carassale@diseg.unige.it
‡ Post-doc, E-mail: andrea.freda@unige.it
‡† Associate Professor, E-mail: giuseppe.piccardo@unige.it

A force model for yawed cylinders, inclusive of buffeting terms as well as basic terms pertinent to galloping and divergence instability, has been proposed by Strømmen and Hjorth-Hansen (1995) on the base of the classical quasi-steady linearized formulation modified by projecting the wind velocity through the "cosine rule". Although such formulation is believed reliable, at least for small yaw angles, since it is derived from the traditional quasi- steady approach, it is unable to predict the instability of circular cylinders.

The open problem concerns with providing a theoretical explanation of the divergent oscillations observed in the wind-tunnel tests and defining a criterion for their prediction. In Cheng, *et al.* (2003a) a modified Den Hartog criterion is proposed to evaluate the critical condition for dry inclined cables, using the derivative of the lift coefficient with respect to the yaw angle (in place of the angle of attack). However, unlike the traditional galloping theory, the proposed criterion is based on only experimental observations. Macdonald and Larose (2004) propose a general expression for the quasi-steady aerodynamic damping of a dry inclined cylinder, but limited to a 1 degree-of-freedom (dof) motion.

The present paper proposes a generalization of the quasi-steady formulation for the definition of the flow-induced forces involving fluid-structure interaction terms acting on yawed and inclined circular cylinders. The objective is to propose a consistent 2 degree-of-freedom theoretical model suitable for representing experimental tests, as those presented in Cheng, *et al.* (2003a, 2003b) and Larose, *et al.* (2003), in which the three-dimensionality of the flow cannot be neglected. Such model makes possible a reliable prediction of the aerodynamic instability of yawed circular cylinders. For this purpose, in the treatment that follows, the expression of the forces is limited to the first-order (linearized forces), though the approach could be extended to include an arbitrary cross-section and a wide class of nonlinear terms deriving from the fluid-structure interaction.

Numerical applications, based on the static aerodynamic coefficients measured by Cheng, *et al.* (2003a), illustrates the potentiality of the proposed model in predicting the critical conditions of yawed circular cylinders. The unstable oscillations observed during the dynamical tests (Cheng, *et al.* 2003a, Larose, *et al.* 2003) are correctly recognized and can be interpreted as a galloping instability. The conclusions summarise the results achieved and discuss the role of the leading parameters in the rise of unstable motions.

2. Model of wind forces on inclined circular cylinders

The present Section introduces the problem of modelling the wind force acting on inclined circular cylinders. The respective directions of wind velocity and cylinder axis are identified through a suitable pair of angles. A model for the definition of the aerodynamic forces is proposed referring first to the case of fixed cylinder in uniform flow and then generalizing the treatment to the case of moving cylinder in turbulent flow. Finally, the influence of the Reynolds number on the instantaneous quantities governing the motion is discussed.

2.1. Reference angles

The formulation of a model of wind forces on inclined cylinders requires, first of all, the identification of a suitable couple of angles defining the attitude of the cylinder towards the wind (Fig. 1). To simplify the discussion, let us consider the practical case of a cable-stayed bridge yawed with respect to the wind direction. Let us consider an orthogonal reference system X_1, X_2, X_3

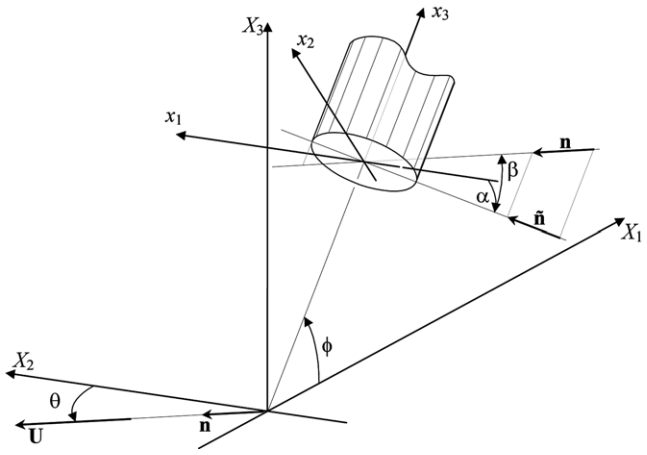

Fig. 1 Identification of the reference angles and of the reference systems

defined orienting X_1 along the bridge axis, and the axis X_3 vertically directed upwards (Fig. 1). Let us consider a cable laying in the plane X_1, X_3 whose axis forms the angle ϕ with X_1 (i.e. with the deck of the bridge). The wind velocity is contained in the horizontal plane and its direction is identified by the unit-vector $\mathbf{n}$ at an angle θ with respect to the axis X_2. The angles ϕ and θ here defined are referred to as inclination and yaw angles; the case $\theta = 0^o$ represents the usual case of bridge in cross-flow conditions, while $\phi = 0^o$ and $\phi = 90^o$ represent, respectively, the ideal limit cases of horizontal and vertical cable.

In order to simplify the modelling of the wind force acting on the cable it is convenient to introduce the local reference system x_1, x_2, x_3 defined letting x_3 be aligned with the cylinder axis and x_1 parallel to X_2. In this way, x_1 and x_2 identify, respectively, the so-called out-of-plane and in-plane directions for the cable displacement. For the purpose of studying the wind action on the cable, the configuration determined by the angles ϕ and θ can be equivalently defined through the angle α between the axis x_1 and the projection $\tilde{\mathbf{n}}$ of $\mathbf{n}$ onto the plane x_1, x_2, and the angle β between $\tilde{\mathbf{n}}$ and $\mathbf{n}$ (Fig. 1). The couples of angles ϕ, θ and α, β are related by the equations (the proof is given in Appendix A):

$$\begin{aligned} \tan\alpha &= \sin\phi \tan\theta \\ \sin\beta &= \cos\phi \sin\theta \end{aligned} \tag{1}$$

Similar expressions have been presented in Larose, *et al.* (2003), but referring to a different definition of the angles.

2.2. Fixed cylinder in uniform flow

Let us consider the circular cylinder previously described and showed in Fig. 2 together with the local reference system x_1, x_2, x_3. With respect to such reference system the unit-vector $\mathbf{n}$ representing the direction of the wind velocity is expressed as:

$$\mathbf{n} = \frac{\mathbf{U}}{\|\mathbf{U}\|} = [\cos\alpha\cos\beta \quad \sin\alpha\cos\beta \quad -\sin\beta]^T \tag{2}$$

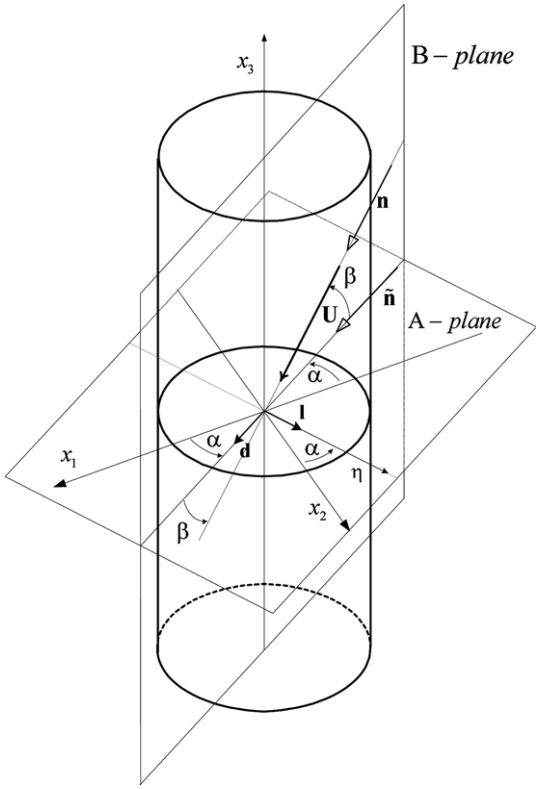

Fig. 2 Three-dimensional representation of the fixed cylinder in uniform flow

where $\|\mathbf{U}\|$ is the Euclidean norm of the wind velocity vector $\mathbf{U}$; the angles α and β describe, respectively, a rotation around x_3 (i.e. in the A-plane represented in Fig. 2) and a rotation around the axis η (i.e. in the B-plane represented in Fig. 2).

The aerodynamic force per unit length acting on the cylinder can be expressed as :

$$\mathbf{f} = \frac{1}{2}\rho b \| \mathbf{U} \|^2 (C_D \mathbf{d} + C_L \mathbf{l}) \tag{3}$$

where ρ is the air density, b is a reference size of the cylinder (e.g. the diameter); C_D and C_L are the drag and lift force coefficients evaluated experimentally measuring the aerodynamic forces or pressures on a fixed cylinder by a wind-tunnel test realized, for example, likewise described by Cheng, *et al.* (2003a); $\mathbf{d}$ and $\mathbf{l}$ are unit-vectors in the plane x_1, x_2 representing the drag and lift directions, defined as:

$$\mathbf{d} = \begin{pmatrix} \cos\alpha \\ \sin\alpha \\ 0 \end{pmatrix} = \frac{1}{\cos\beta}\begin{pmatrix} n_1 \\ n_2 \\ 0 \end{pmatrix}; \qquad \mathbf{l} = \begin{pmatrix} -\sin\alpha \\ \cos\alpha \\ 0 \end{pmatrix} = \frac{1}{\cos\beta}\begin{pmatrix} -n_2 \\ n_1 \\ 0 \end{pmatrix} \tag{4}$$

n_1 and n_2 being the projections of $\mathbf{n}$ along x_1 and x_2, respectively. The force defined by Eq. (3) is

parallel to the plane x_1, x_2, i.e., is orthogonal to the cylinder axis. Actually, the aerodynamic force does have also an axial component, but it is disregarded since it is generally small compared to the others; moreover, its structural effects are usually negligible and its evaluation by a wind-tunnel test is very difficult and uncertain.

The coefficients C_D and C_L depend on the wind direction $\mathbf{n}$ (i.e. on the angles α and β) as well as on the Reynolds number. However, in the present case of circular cylinder, C_D and C_L must be independent of α because of the cross-section symmetry. This simplifies very much the experimental measurements as well as the theoretical formulation leading to the following expression of the force:

$$\mathbf{f} = \frac{1}{2}\rho b \|\mathbf{U}\|^2 \mathbf{C}(\beta)\mathbf{n}\frac{1}{\cos\beta} \tag{5}$$

where

$$\mathbf{C}(\beta) = \begin{bmatrix} C_D(\beta) & -C_L(\beta) & 0 \\ C_L(\beta) & C_D(\beta) & 0 \\ 0 & 0 & 0 \end{bmatrix} \tag{6}$$

2.3. Moving cylinder in turbulent flow

The quasi-steady theory assumes that the flow-induced forces acting on a moving cylinder can be predicted adopting the expression pertinent to a fixed cylinder in which the asymptotic flow velocity is substituted with the flow-cylinder relative velocity. From a physical point of view this means that the forces are determined only by the instantaneous geometry and the instantaneous velocity field of the flow around the cylinder, and that any memory effect is negligible. Such a hypothesis may be satisfied if the characteristic fluid-dynamic time scale of the velocity fluctuations in the wake of the cylinder is much faster than the characteristic time scale of the cylinder oscillation. An explicit expression of this concept may be stated comparing the cylinder oscillation frequency f_c and the vortex-shedding frequency f_w:

$$f_c \ll f_w = \frac{St\|\mathbf{U}\|}{b} \tag{7}$$

where St is the Strouhal number. Following analogous considerations it is possible to take into account also the effect of turbulence in the incoming flow, idealized as a quasi-static perturbation of the asymptotic velocity.

Accepting the validity of the aforementioned hypotheses, the aerodynamic forces acting on a moving cylinder in turbulent flow can be expressed by the model derived for the case of fixed cylinder in uniform flow, substituting the steady wind velocity $\mathbf{U}$ with the instantaneous (function of the time t) flow-cylinder relative velocity $\mathbf{U}^*(t)$ (Fig. 3) defined as:

$$\mathbf{U}^*(t) = \mathbf{U} + \mathbf{u}(t) - \dot{\mathbf{q}}(t) = \|\mathbf{U}\|(\mathbf{n} + \mathbf{z}(t)) \tag{8}$$

where the vectors $\mathbf{u}(t)$ and $\dot{\mathbf{q}}(t)$ collect, respectively, the components of the wind turbulence and of the cylinder velocities along x_1, x_2 and x_3; $\mathbf{z} = (\mathbf{u} - \dot{\mathbf{q}})/\|\mathbf{U}\|$ represents the nondimensional

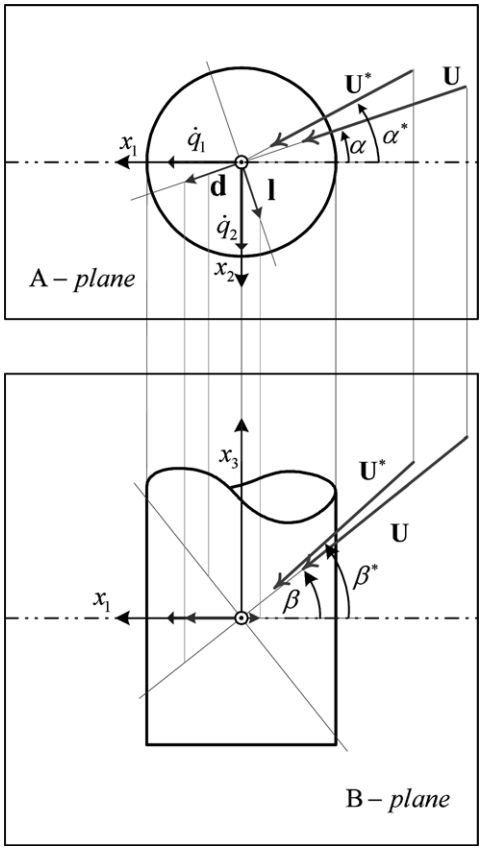

Fig. 3 Moving cylinder in turbulent flow: sections on A-plane (a) and B-plane (b)

instantaneous fluctuation of the relative velocity. The direction of the instantaneous relative velocity is identified by the unit-vector $\mathbf{n}^*$ that is provided by Eq. (2) in which α and β are substituted with the instantaneous angles α^* (Fig. 3(a)) and β^* (Fig. 3(b)).

The instantaneous wind force $\mathbf{f}^*$ is obtained from Eq. (5), substituting $\mathbf{U}$, $\mathbf{n}$, β with their instantaneous counterparts $\mathbf{U}^*$, $\mathbf{n}^*$, β^*:

$$\mathbf{f}^* = \frac{1}{2}\rho b \left\|\mathbf{U}^*\right\|^2 \mathbf{C}(\beta^*)\mathbf{n}^* \frac{1}{\cos\beta^*} \tag{9}$$

where

$$\left\|\mathbf{U}^*\right\| = \|\mathbf{U}\|\|\mathbf{n}+\mathbf{z}\| \tag{10}$$

$$\mathbf{n}^* = \frac{\mathbf{U}^*}{\left\|\mathbf{U}^*\right\|} = \frac{(\mathbf{n}+\mathbf{z})}{\|\mathbf{n}+\mathbf{z}\|} \tag{11}$$

$$\beta^* = -\mathrm{asin}\left(\frac{n_3+z_3}{\|\mathbf{n}+\mathbf{z}\|}\right) \tag{12}$$

in which n_3 and z_3 represents, respectively, the projection of $\mathbf{n}$ and $\mathbf{z}$ along the axis x_3. Substituting Eqs. (10) and (11) into Eq. (9), the instantaneous force can be expressed as:

$$\mathbf{f}^* = \frac{1}{2}\rho b\|\mathbf{U}\|^2 g(\mathbf{z})\mathbf{C}(\beta^*)(\mathbf{n}+\mathbf{z}) \tag{13}$$

where:

$$g(\mathbf{z}) = \|\mathbf{n}+\mathbf{z}\|\frac{1}{\cos(\beta^*(\mathbf{z}))} \tag{14}$$

From the inspection of Eqs. (13), (14) and (12) it can be noted that the instantaneous velocity $\mathbf{f}^*$ depends on time only through vector $\mathbf{z}$. Such a vector, because of its definition, has small modulus, thus $\mathbf{f}^*$ may be represented by the McLaurin series expansion:

$$\begin{aligned}\mathbf{f}^*(\mathbf{z}) &= \mathbf{f}^*(\mathbf{0}) + (\nabla_{\mathbf{z}}^{\mathrm{T}} \otimes \mathbf{f}^*)\big|_{\mathbf{z}=\mathbf{0}}\,\mathbf{z} + \mathrm{O}(\|\mathbf{z}\|^2)\\ &= \mathbf{f}_0 + \mathbf{f}_1\mathbf{z} + \mathrm{O}(\|\mathbf{z}\|^2)\end{aligned} \tag{15}$$

where $\nabla_{\mathbf{z}}^{\mathrm{T}} = [\partial/\partial z_1 \quad \partial/\partial z_2 \quad \partial/\partial z_3]$ and the symbol $\otimes$ represents the Kronecker product (Di Paola, *et al.* 1992). Analogous expansions can be operated for the functions $g(\mathbf{z})$ and $\beta^*(\mathbf{z})$ leading to the expressions:

$$\begin{aligned}g(\mathbf{z}) &= g(\mathbf{0}) + (\nabla_{\mathbf{z}}^{\mathrm{T}} \otimes g)\big|_{\mathbf{z}=\mathbf{0}}\,\mathbf{z} + \mathrm{O}(\|\mathbf{z}\|^2)\\ &= g_0 + g_1\mathbf{z} + \mathrm{O}(\|\mathbf{z}\|^2)\end{aligned} \tag{16}$$

$$\begin{aligned}\beta^*(\mathbf{z}) &= \beta^*(\mathbf{0}) + (\nabla_{\mathbf{z}}^{\mathrm{T}} \otimes \beta^*)\big|_{\mathbf{z}=\mathbf{0}}\,\mathbf{z} + \mathrm{O}(\|\mathbf{z}\|^2)\\ &= \beta_0 + \boldsymbol{\beta}_1\mathbf{z} + \mathrm{O}(\|\mathbf{z}\|^2)\end{aligned} \tag{17}$$

where the quantities g_0, $\mathbf{g}_1$, β_0 and $\boldsymbol{\beta}_1$ are obtained differentiating Eqs. (14) and (12) :

$$\begin{aligned} g_0 &= \frac{1}{\cos\beta}\,; \qquad \mathbf{g}_1 = \left[\cos\alpha(1-\tan^2\beta) \quad \sin\alpha(1-\tan^2\beta) \quad -2\frac{\sin\beta}{\cos\beta}\right]\\ \beta_0 &= \beta\,; \qquad\qquad \boldsymbol{\beta}_1 = [-\cos\alpha\sin\beta \quad -\sin\alpha\sin\beta \quad -\cos\beta\,]\end{aligned} \tag{18}$$

The matrix of the aerodynamic coefficients $\mathbf{C}(\beta^*)$ is expanded in a Taylor series around the static configuration ($\beta^* = \beta$) resulting:

$$\mathbf{C}(\beta^*) = \mathbf{C}(\beta) + \mathbf{C}'(\beta)(\beta^* - \beta) + \mathrm{O}(|\beta^* - \beta|^2) \tag{19}$$

where $\mathbf{C}' = d\mathbf{C}/d\beta$. Substituting Eqs. (15)-(19) into Eq. (13) and equating the terms of the same order it yields:

$$\begin{aligned}\mathbf{f}_0 &= \frac{1}{2}\rho b\|\mathbf{U}\|^2\mathbf{C}(\beta)\mathbf{n}\frac{1}{\cos(\beta)}\\ \mathbf{f}_1 &= \frac{1}{2}\rho b\|\mathbf{U}\|^2[\mathbf{C}(\beta)\mathbf{n}\mathbf{g}_1 + g_0\mathbf{C}'(\beta)\mathbf{n}\boldsymbol{\beta}_1 + g_0\mathbf{C}(\beta)\,]\end{aligned} \tag{20}$$

It is worth noting that the zero-order term of $\mathbf{f}^*$ corresponds to the force $\mathbf{f}$ given in Eq. (5) for the fixed cylinder in uniform flow, while $\mathbf{f}_1\mathbf{z}$ represents its linear correction due to the instantaneous nondimensional relative velocity $\mathbf{z}$.

The Eqs. (15) and (20) provide the expression of the linearized force acting on a circular cylinder moving with velocity $\dot{\mathbf{q}}$ in a turbulent wind flow. In the case of moving cylinder in smooth flow Eqs. (15) and (20) remain valid letting $\mathbf{z} = -\dot{\mathbf{q}} / \|\mathbf{U}\|$.

2.4. Effects due to the instantaneous fluctuation of the relative velocity

In Eq. (13) it is implicitly assumed that the matrix of the aerodynamic coefficients $\mathbf{C}$ changes with the time due to the instantaneous fluctuation of flow-cylinder relative velocity $\mathbf{z}$. Such a variation is obtained by substituting the static angle β between the flow velocity and the cylinder axis with the instantaneous angle β^* (Fig. 3). The model, on the contrary, does not take into account that the velocity fluctuation (and the corresponding Reynolds number fluctuation) may produce a variation of the aerodynamic coefficients as suggested by Macdonald and Larose (2004) for the expression of the aerodynamic damping of a dry inclined cable.

The implementation in the force model of the Reynolds dependency does not produce any mathematical difficulty, indeed it is sufficient to substitute the steady Reynolds number Re with the instantaneous Reynolds number Re^*, corresponding to the velocity fluctuation $\mathbf{z}$, and generalizing Eq. (19) with a bi-variate Taylor series expansion including the derivatives of the aerodynamic coefficients with respect to Re. Actually, while the substitution of β with β^* may be justified fulfilling the condition (7), the substitution of Re with Re^* is supported by a much weaker motivation and can lead to results far from the experimental evidence (Freda 2005). The variation of the aerodynamic coefficients with Re is important only in the critical regime in which C_D has a strongly negative slope. In such condition, however, the dependency between C_D and Re is very complicate and uncertain. In particular, Schewe (1983, 2001), during a wide experimental campaign on fixed circular cylinders in uniform flow, observed a hysteretic behaviour of the drag force with respect to small fluctuations of Re around its critical value. This phenomenon can lead to two consequences that modify significantly the dynamics predicted through the quasi-steady assumption: for small fluctuations of Re (due to the cylinder motion) the drag force may not have any significant variation; the hysteretic behaviour of the drag force produces an additional component of aerodynamic damping of the cylinder.

3. Dynamic instability of an elastic-supported cylinder

Let us consider a rigid circular cylinder oriented with respect to the wind according to the angles α and β, supported at its ends by linear visco-elastic devices oriented along the axes x_1 and x_2. The incoming flow is laminar and homogeneous over the entire length of the cylinder. The cylinder is allowed having only transversal vibrations, i.e., all the points of the cylinder move on planes orthogonal to the cylinder axis (parallel to the plane x_1, x_2); no rotations are allowed. The configuration of the cylinder can be represented by the displacement components q_1 and q_2 of any of its points along the axes x_1 and x_2, respectively. The dynamic equilibrium condition can be written in the form:

$$\ddot{\hat{\mathbf{q}}}(t) + \mathbf{\Gamma}\dot{\hat{\mathbf{q}}}(t) + \mathbf{\Omega}\hat{\mathbf{q}}(t) = \frac{1}{m}\hat{\mathbf{f}}^*(t) \tag{21}$$

where $\hat{\mathbf{q}} = \{q_1, q_2\}^T$ is the displacement vector reduced to the plane x_1, x_2; $\mathbf{\Omega} = \text{diag}(\omega_1, \omega_2)$ and $\mathbf{\Gamma} = 2\text{diag}(\xi_1\omega_1, \xi_2\omega_2)$, ω_j and ξ_j being the circular frequency and damping ratio corresponding to the motion in the direction $j = 1, 2$; m is the mass-per-unit-length of the cylinder; $\hat{\mathbf{f}}^* = \{f_1^*, f_2^*\}^T$ is the vector of the instantaneous force-per-unit-length given by Eqs. (13), reduced to the plane x_1, x_2.

The equation of motion (21) is nonlinear since the wind force $\hat{\mathbf{f}}^*$ depends on the flow-cylinder relative velocity $\mathbf{z}$ and, therefore, of the cylinder response $\dot{\mathbf{q}}$. The study of the instability critical conditions, however, can be performed considering a linearized model of the flow-induced forces disregarding the terms identified as $O(\|\mathbf{z}\|^2)$ in Eq. (15).

Moreover, thanks to the linearity of the left-hand-side of Eq. (21), also the constant term $\mathbf{f}_0$ can be omitted for the evaluation of the critical conditions, leading to the equation:

$$\ddot{\hat{\mathbf{q}}}(t) + \mathbf{\Gamma}\dot{\hat{\mathbf{q}}}(t) + \mathbf{\Omega}\hat{\mathbf{q}}(t) = -\frac{1}{m\|\mathbf{U}\|}\hat{\mathbf{f}}_1\dot{\hat{\mathbf{q}}}(t) \tag{22}$$

where $\hat{\mathbf{f}}_1$ is the reduction to the plane x_1, x_2 of the matrix $\mathbf{f}_1$ given by Eq. (20). Eq. (22) can be rearranged into a state-space formulation, resulting:

$$\dot{\mathbf{y}} = \mathbf{A}\mathbf{y} \tag{23}$$

where

$$\mathbf{y} = \begin{bmatrix} \hat{\mathbf{q}} \\ \dot{\hat{\mathbf{q}}} \end{bmatrix} \qquad \mathbf{A} = \begin{bmatrix} \mathbf{0} & \mathbf{I} \\ -\mathbf{\Omega} & -\left(\mathbf{\Gamma} - \frac{1}{m\|\mathbf{U}\|}\hat{\mathbf{f}}_1\right) \end{bmatrix} \tag{24}$$

in which $\mathbf{0}$ and $\mathbf{I}$ are the zero and identity matrix of order 2×2, respectively.

The dynamical system represented by Eq. (23) is asymptotically stable if and only if all the eigenvalues λ_j ($j = 1, ..., 4$) of the matrix $\mathbf{A}$ lay in the left-half complex plane. A parametric study of the cylinder stability can be therefore performed through a numerical evaluation of the evolution of such eigenvalues with respect to the incoming wind velocity $\|\mathbf{U}\|$ (i.e. the Reynolds number) and the angles α and β.

4. Numerical results

The first objective of this Section is to verify the reliability of the proposed model replicating an experimental dynamical test performed in wind-tunnel. Afterwards, the model permits an exploration of the possible critical conditions in the parameter plane, with particular attention to the detuning parameter and the angle α.

4.1. Replication of a wind-tunnel test

The effectiveness of the model here formulated is verified replicating the dynamical wind-tunnel test described by Cheng, *et al.* (2003a) and Larose, *et al.* (2003), performed in uniform-flow condition. In particular, the setup configurations referred to as 2A and 2C, corresponding, respectively, to the angle pairs $\alpha = 90^o$, $\beta = 30^o$ and $\alpha = 35.3^o$, $\beta = 30^o$ are considered; configuration 2A has been found stable, while configuration 2C experienced galloping-like oscillations at the

velocity $\|\mathbf{U}\| \cong 32$ m/s (Larose, *et al.* 2003), corresponding in such a test to $Re \cong 3.4 \cdot 10^5$. According to the experimental conditions, it is assumed $b = 0.16$ m, $m = 60.8$ kg/m, $\xi = 0.08\%$; the natural circular frequencies are $\omega_1 = 8.796$ rad/s, $\omega_2 = 8.891$ rad/s with a detuning $\sigma = \omega_2/\omega_1 - 1 = 1.08\%$.

In this case, the condition of Eq. (7) for the application of the quasi-steady approach is well fulfilled since $f_c \cong 1.40$ Hz and $f_w \cong 40 - 100$ Hz, having assumed $St \cong 0.2 - 0.5$. Drag and lift coefficients are deduced from the results of the static test described in Cheng, *et al.* (2003a) applying the relationships of Eq. (1) to take into account the different reference system adopted for the angles.

Fig. 4 show the experimental values for the aerodynamic coefficients as presented in Cheng, *et al.* (2003a) together with their polynomial approximation of 6th-order (the drag coefficient is a function of Re and parametric in β, Fig. 4(a); the lift coefficient is a function of β and parametric in

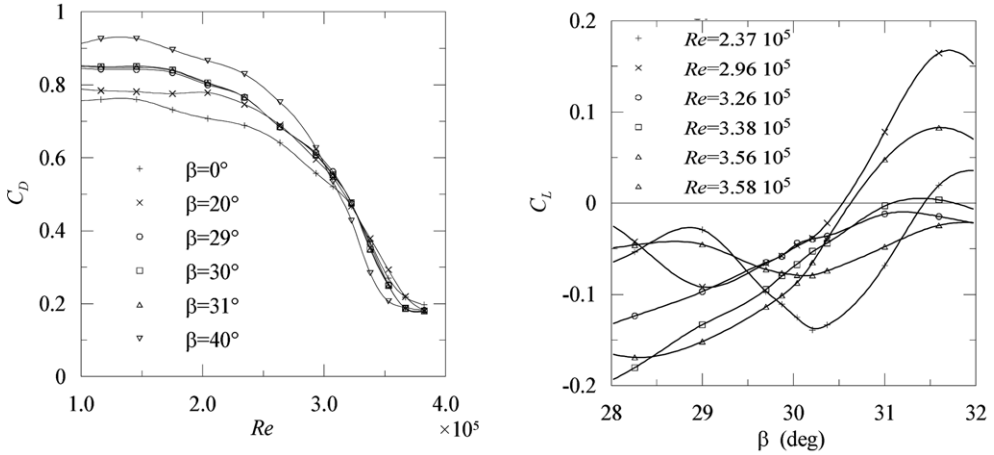

(a) Drag coefficient (b) Lift coefficient

Fig. 4 Experimental values for the aerodynamic coefficients

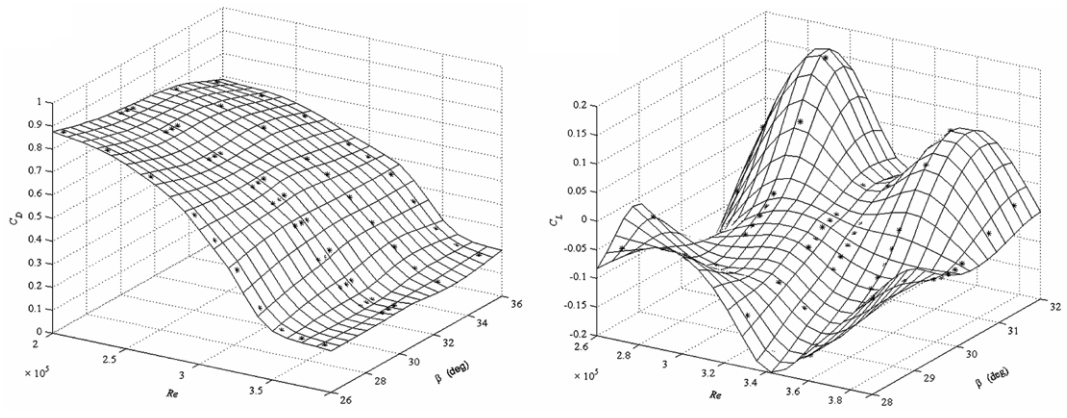

(a) Drag coefficient (b) Lift coefficient

Fig. 5 Regular three-dimensional representation of the aerodynamic coefficients

Re, Fig. 4(b)). In order to use the expressions proposed in Section 2, the aerodynamic coefficients have been represented as regular three-dimensional functions of the β and Re interpolating the

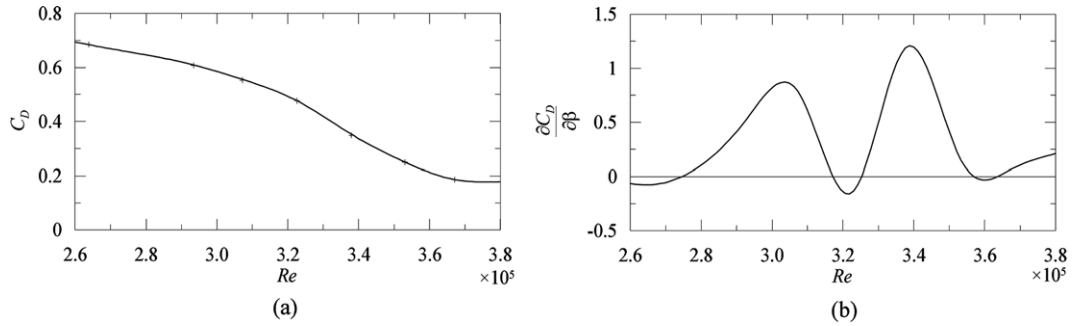

Fig. 6 Drag coefficient and its prime derivative with respect to β (β= 30°)

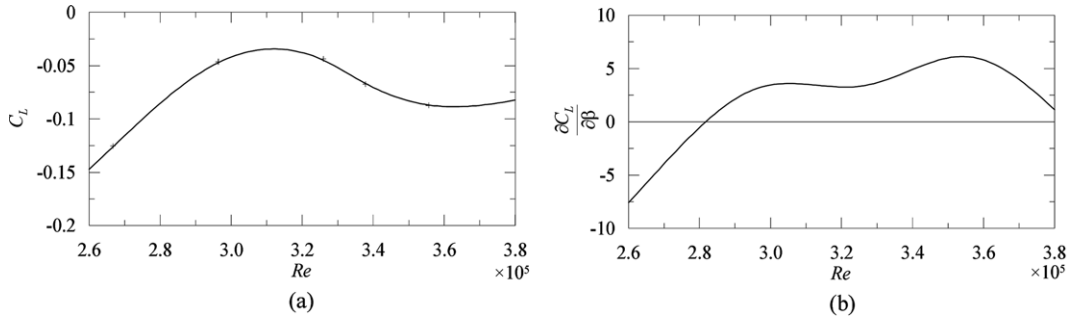

Fig. 7 Lift coefficient and its prime derivative with respect to β (β= 30°)

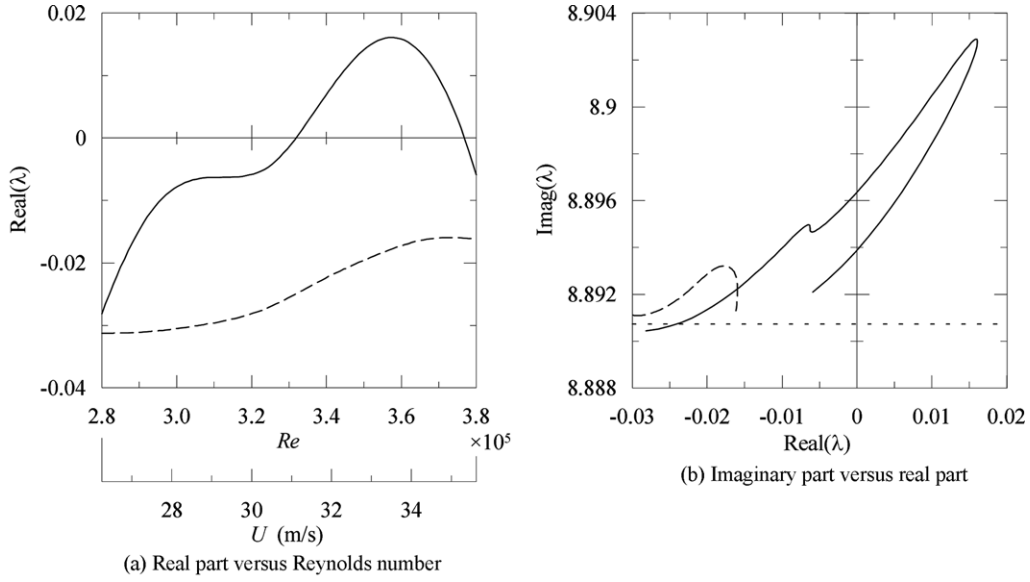

Fig. 8 Critical eigenvalues in the setup configurations 2A (continuous line) and 2C (dashed line)

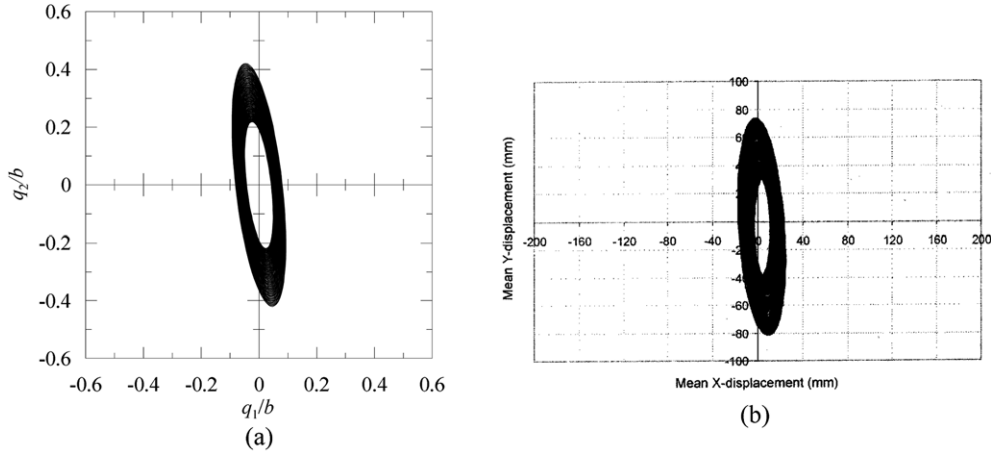

Fig. 9 Galloping-like motions ($Re = 3.4 \cdot 10^5$). Numerical results (a), experimental results presented by Cheng, *et al.* (2003b) ($b = 0.16$ m) (b)

experimental data as shown in Fig. 5. In this way it is easy to deduce the aerodynamic coefficients and their prime derivative with respect to β for $\beta = 30^o$ and $Re \in [2.6 \cdot 10^5,\ 3.8 \cdot 10^5]$ (C_D Fig. 6, C_L Fig. 7). All the numerical results in the sequel are developed keeping constant the angle β (equal to 30^o) coherently with the condition of the experimental dynamic test.

Fig. 8 show the evolution of the critical eigenvalue (the one with maximum real part) as a function of Re in the range $2.8 \cdot 10^5 - 3.8 \cdot 10^5$. In the case of $\alpha = 35.3^o$ (solid line) the critical eigenvalue crosses the imaginary axis at a Reynolds number slightly larger than $3.3 \cdot 10^5$ (Fig. 8(a)) predicting a galloping-like instable behaviour in excellent accord with the experimentation ($Re = 3.4 \cdot 10^5$); the eigenvalue returns in the left-half complex plane for $Re \cong 3.75 \cdot 10^5$. In the case of $\alpha = 90^o$, in which no instability was observed (dashed line) all the eigenvalues remain in the left-half complex plane. The Fig. 8(b) shows the evolution of the real and imaginary parts of the critical eigenvalues; the oscillation frequencies slightly change when unstable motion appears.

Fig. 9 show trajectories of the cylinder (in the plane x_1, x_2) for the case $\alpha = 35.3^o$, $\beta = 30^o$, $Re = 3.4 \cdot 10^5$. The motion is characterized by elliptical orbits involving displacements along both the axes x_1 and x_2, with a prevalent direction of motion inclined of approximately 7^o with respect to the axis x_2. Again, the behaviour predicted by the theoretical model (Fig. 9(a)) is very close to the experimental results presented in Cheng, *et al.* (2003b) (Fig. 9(b)).

4.2. Effects of detuning and α-angle on critical conditions

Passing to investigating the critical conditions when the reference angle α is varying, Fig. 10 shows a contour plot of the real part of the critical eigenvalue in the plane α-Re for the case $\beta = 30^o$ keeping constant the detuning σ. It can be note that, in such condition, instability can occur within a range of α between 10^o and 75^o, approximately. Moreover, all this kind of bifurcations appear as confined since the system can regain stability (i.e. the real part of the critical eigenvalue becomes negative) for a sufficiently high value of the Reynolds number (transient instability).

The influence of detuning is highlighted by Fig. 11, where the trajectories of the cylinder,

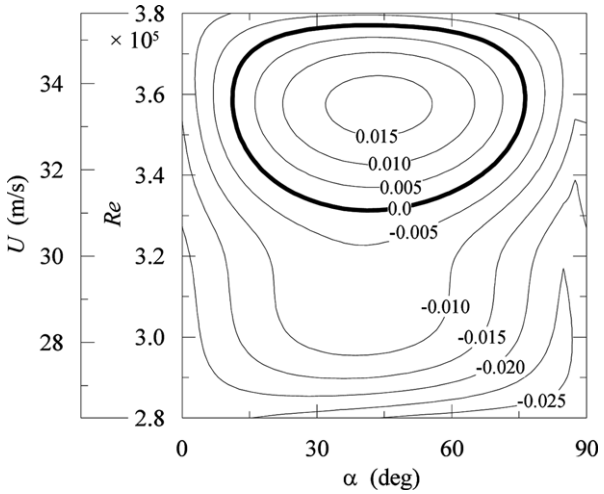

Fig. 10 Influence of the angle α on critical conditions

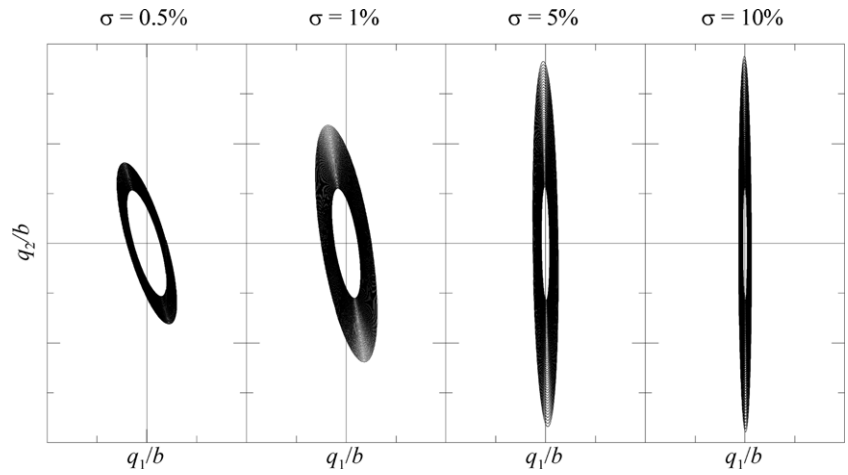

Fig. 11 Influence of detuning parameter σ on galloping motion ($Re = 3.57 \cdot 10^5$)

evaluated for the case $\alpha = 35.3°$, $\beta = 30°$ at $Re = 3.57 \cdot 10^5$, are shown for different values of the detuning ($\sigma = 0.5\%$, 1%, 5%, 10%). It can be noted that, for small detuning the motion involves both the two dof's producing wide orbits with the characteristic inclination observed in the experimental tests (see Fig. 9); for large detuning, instead, instability involves only one dof (in the present case q_2, but it depends on the angles α and β, Freda 2005), the orbit becomes thinner and oriented along one of the principal axes of the stiffness matrix (i.e. the directions of the spring supports, assumed orthogonal each other). In such a case, a single-dof modelling of the dynamics may lead to a correct evaluation of the critical velocity, even if no criterion is available to predict, a priori, which one of the two dof's is going to experience instability.

Fig. 12 shows the value of the Reynolds number for which the critical eigenvalue crosses the imaginary axis versus the detuning σ for the case $\alpha = 35.3°$, $\beta = 30°$. For low detuning ($|\sigma| < 0.2\%$) instability does not occur due to the coupling between the two dof's. A similar phenomenon has

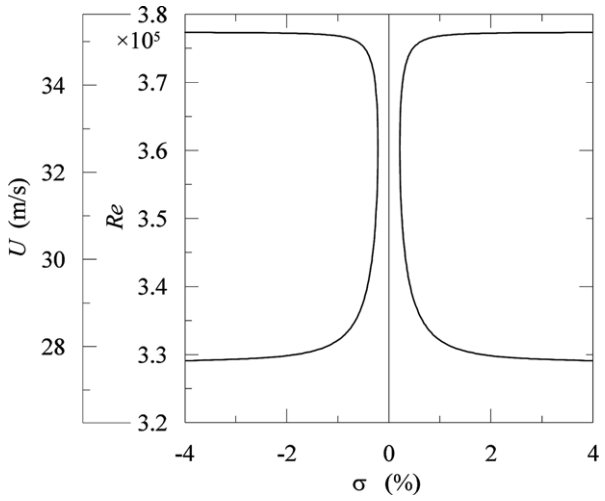

Fig. 12 Influence of detuning parameter σ on critical conditions

been found in classic galloping cases, where it can be proved that cross-sections that are unstable in a single vertical dof schematization, possibly become stable if the horizontal dof is introduced in the model (Luongo and Piccardo 2005). For $|\sigma|>2-4\%$ the instability critical velocity is substantially independent of σ since instability virtually involves only one dof. In intermediate conditions the instability critical velocity is quite influenced by the detuning, which governs the coupling between the two oscillation modes.

5. Conclusions

In this paper a theoretical quasi-steady model able to reproduce the flow-induced forces on yawed dry circular cylinders is proposed. This formulation presents some differences with respect to the literature, where the problem has been treated in a simplified way and solutions are proposed for the case of one dof only. The following conclusions can be drawn.

(1) The model of forces is developed in vector notation, using concepts derived from the Kronecker algebra, which permit to obtain concise expression (for non linear components of forces too) and to easily use symbolic manipulation software.
(2) The proposed theoretical model seems able to reproduce the actual instability behaviours, as those found during wind tunnel tests. It appears that circular cylinder instability occurs for particular combinations of the angles β (angle between the wind direction and the normal to the cylinder axis) and α (rotation of the cylinder around its own axis), within certain ranges of the Reynolds number.
(3) The implementation in the force model of the Reynolds dependency does not involve any mathematical difficulty, but requires further investigation under the physical point of view.
(4) The angle α is meaningful only if the mechanical characteristics of the support devices present differences, even though very small. This confirms the extreme sensitivity recognized in former experiments where the phenomenon "occur or fails to occur with even slight differences in support conditions" (Saito, *et al.* 1994).
(5) The numerical results highlights the existence of a region in the plane α-Re in which the

bifurcation phenomenon occurs; this results could be act as a guide for new experimental tests. It should be noted that all the bifurcations are of transient type (i.e. the system regains stability when wind velocity increases).

(6) The detuning parameter appears as fundamental in order to obtain the instability phenomenon. This aspect has been already found in classic galloping cases, where the aerodynamic coefficients are constant with respect to the Reynolds number. The presence of a small detuning can significantly differ from the case of large detuning (i.e. predominance of a sole dof).

(7) The (initial) trajectories on the configuration plane are elliptical spirals, more or less flat depending on the detuning parameter σ. For small detuning the motion involves both the two degree-of-freedom producing wider orbits in excellent agreement with those observed during the experimental tests.

(8) The proposed model is specifically oriented to the simulation of inclined cables for which the detuning parameter is usually small. In such a case, single-dof modelling appears inadequate since instability is governed by the dof's coupling. In the described example the single-dof model provides a lower bound for the critical velocity, but fails in the case of very-low detuning predicting an instability that does not occur.

(9) The proposed model has been applied only in cases of uniform flow, even if it has been consistently derived including turbulent flow components. The validation of the model in turbulent-flow condition, however, is not automatically assured, since the fluid-dynamic phenomena giving rise to instability could deeply change with high turbulence intensity. Experimental investigations in this field seems necessary to proceed further with the theoretical modelling.

Acknowledgements

This study has been partially supported by the Italian Ministry of University (MIUR) through a co-financed program PRIN.

Appendix A – Relationships between reference angles

The present Appendix provides a proof for the relationships given in Eqs. (1) between the two couples of reference angles ϕ, θ and α, β shown in Fig. 1 representing the wind direction with respect to the global reference system X_1, X_2, X_3 and the cylinder reference system x_1, x_2, x_3, respectively. The axes of such reference systems are identified, respectively, by the unit-vectors $\mathbf{e}_1$, $\mathbf{e}_2$, $\mathbf{e}_3$ and $\mathbf{f}_1$, $\mathbf{f}_2$, $\mathbf{f}_3$. By inspecting Fig. 1 the following relationships can be easily proved:

$$\begin{aligned} \mathbf{f}_1 &= \mathbf{e}_2 \\ \mathbf{f}_2 &= -\sin\phi\,\mathbf{e}_1 + \cos\phi\,\mathbf{e}_3 \\ \mathbf{f}_3 &= \cos\phi\,\mathbf{e}_1 + \sin\phi\,\mathbf{e}_3 \end{aligned} \tag{25}$$

The unit-vector $\mathbf{n}$ representing the flow direction and its projection $\tilde{\mathbf{n}}$ on the plane x_1, x_2 are given by the relationships:

$$\begin{aligned} \mathbf{n} &= -\sin\theta\,\mathbf{e}_1 + \cos\theta\,\mathbf{e}_2 \\ \tilde{\mathbf{n}} &= \mathbf{n} - (\mathbf{n}\cdot\mathbf{f}_3)\mathbf{f}_3 \end{aligned} \tag{26}$$

where $\cdot$ represents the inner product in $\Re^3$.

The first of Eqs. (1) can be proved noting that the vectors $\mathbf{f}_1$, $\mathbf{f}_2$ and $\tilde{\mathbf{n}}$ are coplanar and that the tangent of the angle α can be expressed by the formula:

$$\tan \alpha = \frac{\tilde{\mathbf{n}} \cdot \mathbf{f}_2}{\tilde{\mathbf{n}} \cdot \mathbf{f}_1} \tag{27}$$

that can be expressed in the form of Eqs. (1) through the substitution of Eqs. (25) and (26). Analogously, the second of Eqs. (1) can be proved noting that the vectors $\mathbf{n}$, $\tilde{\mathbf{n}}$ and $\mathbf{f}_3$ are coplanar and that the sine of the angle β is given by the formula:

$$\sin \beta = -\mathbf{n} \cdot \mathbf{f}_3 \tag{28}$$

that can be expressed in the form of Eqs. (1) by using the third one of Eqs. (25) and the first one of Eqs. (26).

References

Cheng, S., Irwin, P.A., Jakobsen, J.B., Lankin, J., Larose, G.L., Savage, M.G., Tanaka, H. and Zurell, C. (2003a), "Divergent motion of cables exposed to skewed wind", *Proceedings of the Fifth Int. Symposium on Cable Dynamics*, S. Margherita Ligure (Italy), September 2003, 271-278.

Cheng, S., Larose, G.L., Savage, M.G. and Tanaka, H. (2003b), "Aerodynamic behaviour of an inclined circular cylinder", *Wind and Struct.*, **6**, 197-208.

Di Paola, M., Falsone, G. and Pirrotta, A. (1992), "Stochastic response analysis of nonlinear systems under Gaussian inputs", *Probabilistic Engineering Mechanics*, **7**, 15-21.

Freda, A. (2005), *Behaviour of Slender Structural Elements Having an Arbitrary Attitude in the Wind Field*, Ph.D. thesis, University of Genova.

Larose, G.L., Jakobsen, J.B. and Savage, M.G. (2003), "Wind-tunnel experiments on an inclined and yawed stay cable model in the critical Reynolds number range", *Proceedings of the Fifth Int. Symposium on Cable Dynamics*, S. Margherita Ligure (Italy), September 2003, 279-286.

Luongo, A. and Piccardo, G. (2005), "Linear instability mechanisms for coupled translational galloping", *J. Sound Vib.*, in press.

Macdonald, J.H.G. and Larose, G.L. (2004), "Quasi-steady analysis of dry inclined cable galloping in the critical Reynolds number range", *Proceedings of WES2004*, UK Wind Engineering Society, Cranfield (UK), September 2004.

Matsumoto, M., Shiraishi, N., Kitazawa, M., Knisely, C., Shirato, H., Kim, Y. and Tsujii, M. (1990), "Aerodynamic behavior of inclined circular cylinders - cable aerodynamics", *J. Wind Eng. Ind. Aerodyn.*, **33**, 63-72.

Saito, T., Matsumoto, M. and Kitazawa, M. (1994), "Rain-wind excitation of cables on cable-stayed Higashi-Kobe Bridge and cable vibration control", *Proceedings of the Int. Conf. Cable-Stayed and Suspension Bridges*, Deauville, October 1994, **2**, 507-514.

Schewe, G. (1983), "On the force fluctuations acting on a circular cylinder in crossflow from subcritical up to transcritical Reynolds numbers", *J. Fluid Mech.*, **133**, 265-285.

Schewe, G. (2001), "Reynolds-number effects in flow around more-or-less bluff bodies", *J. Wind Eng. Ind. Aerodyn.*, **89**, 1267-1289.

Strømmen, E. and Hjorth-Hansen, E. (1995), "The buffeting wind loading of structural members at an arbitrary attitude in the flow", *J. Wind Eng. Ind. Aerodyn.*, **56**, 267-290.

GS